Coherent imaging at 2.4 THz with a CW quantum cascade laser transmitter

Andriy A. Danylov[*a], Thomas M. Goyette[a], Jerry Waldman[a], Michael J. Coulombe[a],
Andrew J. Gatesman[a], Robert H.Giles[a] , Xifeng Qian[b], Neelima Chandrayan[b],
Shivashankar Vangala[b], Krongtip Termkoa[b], William D. Goodhue[b], and William E. Nixon[c].
[a]Submillimeter-Wave Technology Laboratory, University of Massachusetts Lowell,
Lowell, Massachusetts, 01854;
[b]Photonics Center, University of Massachusetts Lowell, Lowell, Massachusetts, 01854;
[c]U.S. Army National Ground Intelligence Center, Charlottesville, Virginia 22911

Abstract

A coherent transceiver using a THz quantum cascade laser as the transmitter and an optically pumped molecular laser as the local oscillator has been used, with a pair of Schottky diode mixers in the receiver and reference channels, to acquire high-resolution images of fully illuminated targets, including scale models. Phase stability of the received signal, sufficient to allow coherent image processing of the rotating target (in azimuth and elevation), was obtained by frequency-locking the TQCL to the free-running, highly stable optically pumped molecular laser. While the range to the target was limited by the available TQCL power (several hundred microwatts) and reasonably strong indoor atmospheric attenuation at 2.408 THz (2.0 dB/m at 40% RH), the coherence length of the QCL transmitter will allow coherent imaging over distances up to several hundred meters. In contrast to non-coherent heterodyne detection, coherent imaging allows signal integration over time intervals considerably longer than the reciprocal of the source, or signal bandwidth, with consequent improvement in the signal-to-noise ratio. Image data obtained with the system will be presented.

Keywords: THz quantum cascade laser, THz imaging, radar cross-section, transmitter, receiver, mixer, coherent detection

1.   Introduction

Based on the well-established principles of electromagnetic similitude[1], the U.S. Army National Ground Intelligence Center (NGIC) Expert Radar Signature Solutions Program (ERADS) has pioneered the application of coherent terahertz (THz) transceiver systems for the production of microwave and millimeter wave radar signature data from highly accurate scale models. Typically, model targets are illuminated with a planar phase front beam using the compact range configuration, thereby establishing a far-field measurement condition. At lower frequencies (160 GHz to approximately 600 GHz) harmonics of amplified and multiplied microwave signals have been successfully used[2-3], and at higher frequencies (above 1.0 THz) CO_2 optically pumped molecular gas lasers (OPL) have been employed[4] as transmitter and local oscillator (LO) sources. These systems have been designed and built by the UMass Lowell Submillimeter-Wave Technology Laboratory (STL) under NGIC sponsorship.

The schematic of a 1.56 THz fully-polarimetric, OPL-based radar system is shown in Fig. 1 (taken from reference 4). High-frequency Schottky diode mixers are used as (1), downconverters for detection and signal processing, and (2), as sideband generators for producing the transmitter bandwidth required for range resolution on the target. Such a system costs roughly $1M to assemble. In addition to the cost of acquiring and maintaining the dual CO_2/OPL lasers, high-frequency mixers and associated electronics, the transceiver depicted in Fig. 1 occupies a 100 ft^2 area and consumes several kW of power while operating. The motivation for identifying simpler and more compact THz sources that can perform transmitter and LO roles is clear.

[*]andriy_danylov@student.uml.edu; phone 1 978-934-1300; fax 1 978-452-3333; stl.uml.edu

Report Documentation Page

1. REPORT DATE **JAN 2010**	2. REPORT TYPE	3. DATES COVERED **00-00-2010 to 00-00-2010**

4. TITLE AND SUBTITLE **Coherent imaging at 2.4 THz with a CW quantum cascade laser transmitter**	5a. CONTRACT NUMBER
	5b. GRANT NUMBER
	5c. PROGRAM ELEMENT NUMBER
6. AUTHOR(S)	5d. PROJECT NUMBER
	5e. TASK NUMBER
	5f. WORK UNIT NUMBER
7. PERFORMING ORGANIZATION NAME(S) AND ADDRESS(ES) **U.S. Army National Ground Intelligence Center,Charlottesville,VA,22911**	8. PERFORMING ORGANIZATION REPORT NUMBER
9. SPONSORING/MONITORING AGENCY NAME(S) AND ADDRESS(ES)	10. SPONSOR/MONITOR'S ACRONYM(S)
	11. SPONSOR/MONITOR'S REPORT NUMBER(S)

12. DISTRIBUTION/AVAILABILITY STATEMENT
Approved for public release; distribution unlimited

13. SUPPLEMENTARY NOTES
in Terahertz Technology and Applications III, Proceedings of SPIE Vol. 7601 (SPIE, Bellingham, WA 2010) January 2010.

14. ABSTRACT

A coherent transceiver using a THz quantum cascade laser as the transmitter and an optically pumped molecular laser as the local oscillator has been used, with a pair of Schottky diode mixers in the receiver and reference channels, to acquire high-resolution images of fully illuminated targets, including scale models. Phase stability of the received signal sufficient to allow coherent image processing of the rotating target (in azimuth and elevation), was obtained by frequency-locking the TQCL to the free-running, highly stable optically pumped molecular laser. While the range to the target was limited by the available TQCL power (several hundred microwatts) and reasonably strong indoor atmospheric attenuation at 2.408 THz (2.0 dB/m at 40% RH), the coherence length of the QCL transmitter will allow coherent imaging over distances up to several hundred meters. In contrast to non-coherent heterodyne detection, coherent imaging allows signal integration over time intervals considerably longer than the reciprocal of the source, or signal bandwidth, with consequent improvement in the signal-to-noise ratio. Image data obtained with the system will be presented.

15. SUBJECT TERMS

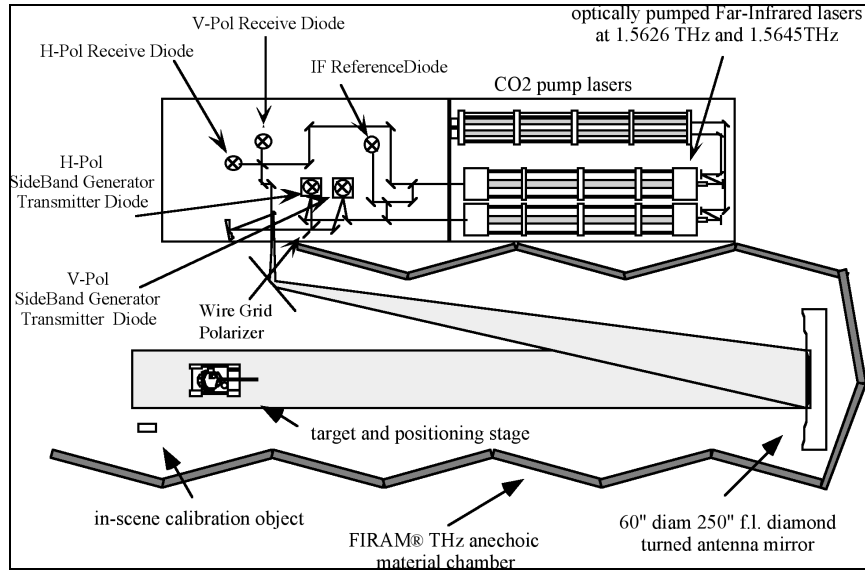| 16. SECURITY CLASSIFICATION OF:			17. LIMITATION OF ABSTRACT	18. NUMBER OF PAGES	19a. NAME OF RESPONSIBLE PERSON
a. REPORT **unclassified**	b. ABSTRACT **unclassified**	c. THIS PAGE **unclassified**	**Same as Report (SAR)**	**8**	

Figure. 1. Diagram of the 1.56 THz compact range with an OPL transmitter and an OPL LO .

THz quantum cascade lasers (TQCLs) offer a promising alternative to the CO_2-driven OPLs as both transmitter and local oscillator (LO) sources in these systems. Implementation of a TQCL would reduce system cost by at least an order of magnitude and sources size from 50 square feet to a size of cryogenic system needed for maintaining a TQCL transmitter and LO. The dramatic reduction in size and cost would open this technology for new applications. The current limitations of TQCLs for this application, as well as ongoing progress in addressing key issues has recently been reviewed[5]. The work reported in this paper, building on advances in source frequency stabilization[6], represents a first step for TQCL insertion into such systems. Using room temperature Schottky diode mixers as receivers and a CH_2DOH molecular laser line at $\nu_{OPL} = 2.409293$ THz as a LO, two dimensional (azimuth/elevation) synthetic aperture imaging of objects has been demonstrated with a $\nu_{QCL} = 2.408293$ (nominal) THz transmitter. Image results are shown along with a description of the relevant features of the hybrid QCL/OPL radar system.

2. THz Imaging Methods

The initial demonstration of QCL operation at THz frequencies in 2002 has been followed by a number of publications on THz imaging applications[7-12] using QCL sources. The imaging configurations have usually involved focusing the TQCL beam to a diffraction-limited spot and scanning the target (spot) across the spot (target). In some instances[11-12] an infrared microbolometer array has supplanted spot scanning. These configurations are useful for illustrating relevant features of THz radiation, e.g., its ability to penetrate certain materials, and simultaneously provide sub-millimeter spatial resolution. However, they are incompatible with the requirements of high-resolution remote sensing, where the term "remote sensing" (taking into account the severe atmospheric absorption at THz frequencies) implies distances on the order of tens of meters. Consider the following set of not unreasonable specifications; an object of interest, 20 m distant from the transceiver, is to be imaged at 1.5 THz with a spatial resolution of 1 mm. Since the angular resolution limit, α, of a receiver aperture is $\alpha = 1.22\,\lambda/d$, where d is the diameter of the receiver aperture, a 5 m diameter dish would be required.

The alternative to unacceptably large real apertures for high-resolution remote sensing at longer wavelengths is to create a synthetic aperture, which generally involves the measurement of phase as well as amplitude. At microwave frequencies synthetic aperture techniques are a necessity for imaging remotely located targets[13] and synthetic aperture radars (SAR) are now widely used, e.g., on UAVs. In a typical SAR system a small transmitter antenna on an airborne platform moves in a horizontal plane, approximately perpendicular to the line-of-sight to the target, while the frequency of the source is swept. Processing, by Fourier transformation, the phase and amplitude of the signal backscattered from the target, provides a two-dimensional (2D) azimuth/range image of scattering centers, where azimuth refers to the horizontal cross-range of a scatterer, and range refers to its distance from the transmitter, measured along the line-of-

sight. Equivalent results can be obtained by holding the antenna fixed, while rotating the target in azimuth. This inverse SAR (ISAR) method is widely used in microwave radar ranges. ERADS compact ranges, such as the 1.56 THz range depicted in Fig. 1, are designed to produce ISAR data from scale model targets.

The ISAR approach can also be applied to produce azimuth/elevation (az/el) images by collecting complex (phase and amplitude) data while rotating the target both in azimuth and elevation. Such 2D THz images can be quite similar to conventional optical imagery when the target's surface is macroscopically rough, i.e. a surface with many discontinuities, and are obtained with a monochromatic source, i.e. no frequency tuning is necessary[14]. 3D THz ISAR imagery also has been demonstrated by combining az/el rotation and frequency tuning[4]. Central to these types of measurements is the frequency stability of the radiation sources, particularly the transmitter. A shift in phase of the signal returned from the target due to an uncontrolled shift in frequency introduces noise and reduces the resolution of the processed image. For near noise-free imagery the phase shift should not exceed several degrees. The phase shift, $\Delta\phi$, (in degrees) due to a frequency shift, Δv, is given by, $\Delta\phi = 360 D \Delta v / c$, where D is the round-trip distance to the target and c is the speed of light. For ERADS compact radar ranges D ~ 25 m. If we require $\Delta\phi \leq 3°$, then $\Delta v \leq 10^5$ Hz. Thus, sources with a frequency jitter of $\pm$ 50 kHz or less are required for coherent image processing. Well designed OPL systems, such as depicted in Fig. 1, can meet this requirement, with ultrastable CO_2 pump lasers and THz laser cavities located in a low-vibration environment.

3. Coherent Imaging with a TQCL Transmitter

Quantum cascade lasers have a high degree of temporal coherence, much greater than conventional semiconductor lasers[15], a result which has been established at mid-infrared[16] and THz[17] frequencies, thus TQCLs should be suitable for coherent THz imaging applications. To overcome the frequency sensitivity of TQCLs to current and temperature fluctuations, several groups have stabilized the laser frequency by locking to a more stable external reference source[18-21]. STL has locked a TQCL to an OPL and achieved a 4 kHz (3dB) linewidth in the (nominal) 1 GHz beat frequency between the two sources[6]. While this is not the desired long-term solution for stabilizing TQCLs, since the goal is to ultimately replace OPLs, the insertion of a locked TQCL transmitter into a coherent imaging system provides, for the first time, an opportunity to evaluate its effectiveness.

In addition to locking the TQCL, the OPL was also used as the LO source to drive a reference Schottky diode mixer and the receiver mixer. THz Schottky diode mixers are preferred to superconducting HEB mixers because of their larger bandwidth and room-temperature operation. However, they require a combination of power level and spatial coherence that has not yet been demonstrated by TQCLs, whereas good HEB mixer noise temperatures have been obtained when driven by TQCLs[20, 22].

The target can be illuminated by a collimated, plane phase front wave, or a spherical wave. The former simulates a true far-field configuration, where the target is effectively in the far field of the outgoing beam and the receive antenna is in the far field of the radiation pattern scattered from the target. Unfortunately, the TQCL beam pattern, after collimation with a 12 inch diameter, 36 inch focal length spherical mirror, was sufficiently non-uniform that portions of the target were poorly illuminated, so the simpler configuration of a diverging spherical wave was used.

The TQCL (2.408 THz, 1 mW of maximum optical power) that was used as a transmitter was grown by UMass Lowell's Photonics Center, and fully characterized by STL. The details can be found in Ref. [23, 24]. The laser had a 4 mm cavity length and a 200 μm waveguide ridge width. It was mounted in a liquid-helium (LHe) dewar to keep the ambient device temperature at about 5 K. A hollow dielectric Pyrex tube of 30 mm length and 1.5 mm inner diameter was used to significantly improve the laser radiation transverse mode content to a near-Gaussian beam profile[23]. The CW TQCL was operated at 3.6 V (478 mA), approximately 0.2 V above threshold, to maintain the laser output to a single-longitudinal mode. The laser was driven by a 6 V battery through a 15 Ω potentiometer.

A very stable CO_2 laser-pumped molecular laser (OPL), operating on the 2409.293 GHz line of CH_2DOH was employed as the LO. Its output power was approximately 100 mW, and a linewidth of 20-30 kHz was due to mechanical and acoustic-induced laser cavity perturbations.
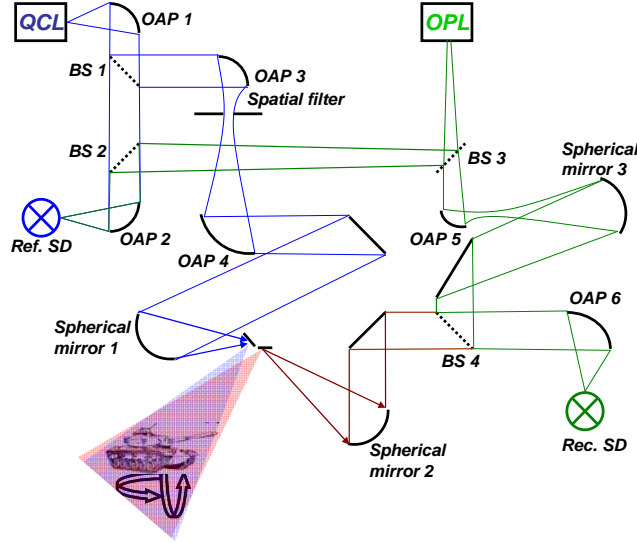
Figure. 2. Schematic of a QCL-based THz transmitter/receiver system for ISAR imaging measurements.

The optical part of the experimental configuration is shown schematically in Fig. 2. The OPL beam, propagating in free space, was split by beam splitter 3 (BS3) and illuminated the reference Schottky diode (Ref. SD), and also drove the receive mixer (Rec. SD) after a beam expansion with spherical mirror 3 and OAP 5. The room temperature mixers were corner-cube mounted, whisker contacted high-frequency Schottky diodes type 1T17, made by University of Virginia. The CW frequency-locked THz QCL (the transmitter) radiation with frequency approximately 1.048 GHz below the frequency of the gas laser was also split with BS1 and a portion illuminated the Ref. SD while the rest was beam expanded with OAPs 3 and 4. The beam profile was cleaned with a spatial filter, and directed towards the target, which was fully illuminated by the beam with a spherical phase front (near-field configuration measurements). The radiation backscattered from the target at a bistatic angle of 1.8º was directed to the receive mixer where it was combined with the OPL radiation using BS 4. This near-monostatic configuration has been the standard design of many microwave radar ranges. The total pathlength of the transmitter radiation from the source to the receiver is about 5.5 m. The powers of the TQCL and the gas laser beams incident on the Ref. SD were about 130 μW and 3 mW, respectively. The Rec. SD was pumped with approximately 13 mW of OPL power.

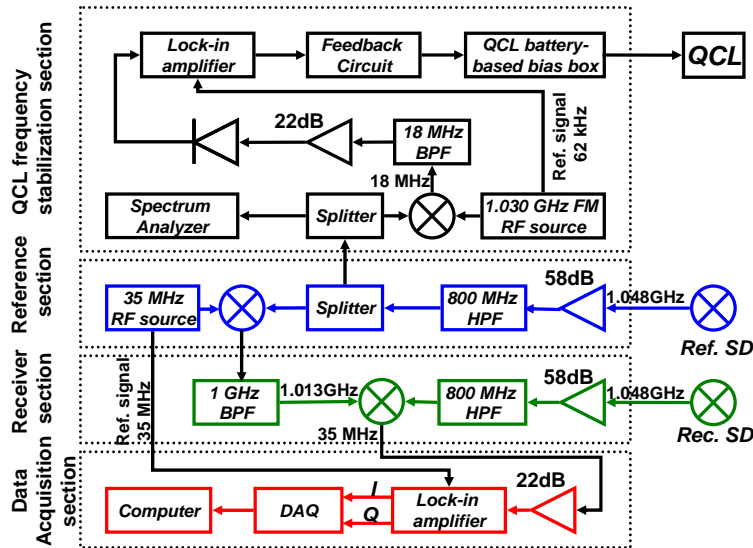The block diagram of the electronic section of the experiment is shown in Fig. 3.

Figure. 3. Circuit configuration used in the system to acquire amplitude (I) and phase (Q)
of a backscattered signal from a target and to lock the TQCL frequency to the OPL reference source.

The intermediate frequency (IF) of 1.048 GHz, ($\nu_{transmitter}$ -ν_{LO}), of both the reference and receive mixers was amplified (58 dB) and high-pass filtered. The Ref. SD 1.048 GHz signal was then mixed with a 35 MHz signal to generate sidebands. The first-order lower sideband was selected with a narrowband filter (25 MHz wide) and mixed with the 1.048 GHz receiver signal to transfer the amplitude and phase information of the signal scattered from the target to carrier frequency of 35 MHz. The 35 MHz signal was processed by a lock-in amplifier to produce amplitude and phase data. At the same time, part of the reference IF signal was used to stabilize the TQCL frequency to the OPL, achieving a QCL linewidth of about 20-30 kHz as described in Ref. [6].

The target was mounted on a stepper-motor-driven rotary stage, for rotation about a vertical axis. The rotary stage was cradled in a goniometer mount, for rotation about a horizontal axis. The positioning accuracy of the system was better than 0.005° in both azimuth and elevation. The stage was 42 inches from the focus of the diverging spherical wave. The object centered about the axis of azimuth rotation and elevated above the elevation axis was rotated around the azimuth axis and pairs of amplitude and phase were recorded at evenly spaced intervals. Then elevation increment was followed and the process was repeated until a "two dimensional window" was swept out in angle as indicated schematically in Fig. 2.

The phase change of a rotated scatterer is proportional to the cross-range distance from the center of rotation. If the phase of the scatterer is measured over a finite angle, then a Fourier Transform can calculate the cross-range coordinate of the scatterer. Following data collection, Fast Fourier Transform (FFT) processing of a series of the back-scattered values collected across a two dimensional angular window convert the data into an angular Doppler-shifted image. This az/el image resembles a photograph of the physical object being measured.

The phase change of any scatterer must not exceed 90° after each incremental step, which is required by the Nyquist criterion for the FFT processing to prevent under sampling. This requirement determines the unambiguous cross range (UCR) and the maximum diameter of the object to be scanned. The UCR (diameter) is defined by

$$D_{UCR} = \lambda \Big/ 2\Theta_{increment} \qquad (1)$$

The image resolution as a function of the total angular extent of the scan is defined by

$$\Delta R = \lambda \Big/ 2\Theta_{Integrated} \qquad (2)$$

4. Results

Imaging radar systems depend on amplitude and phase stability of the signal returned from a target. The amplitude stability of the OPL and the QCL is not an issue and it is within 0.3%. However, the phase stability must be diagnosed because the frequency stabilization technique was applied to the QCL. The signal phase stability for a 40-min period is presented in Fig. 4. This data was collected by measuring the phase of the signal returned from a stationary dihedral positioned at the center of the transmitter beam at the target location. As it can be seen the maximum phase excursion does not exceed approximately ± 7 degrees, which is small enough to create distortion free images because it is much smaller than the phase change generated by a scatterer within the UCR, scanned over a few degrees in azimuth or elevation.
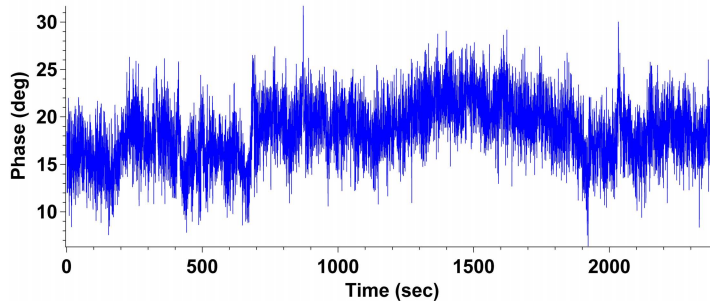

Figure 4. Phase stability of the transceiver over a 40-min period.

Figure 5a is a photograph of a 1/72nd scale model of a T-80BV tank. The result of the 2.4 THz az/el imaging on this scale model is shown in Fig. 5b. The amplitude values in dB are represented in colors on a logarithmic color scale. The

data were recorded from -2º to 3.8º in elevation and from -4.8º to 4.8º in azimuth with an angular spacing of 0.028º in elevation and 0.02º in azimuth, assuming that both angles are zero when the tank's broadside is normal to the transmitter beam propagation direction. Since the maximum velocity of the rotary stage was 2.4 degrees/sec, it took about 40 min to acquire the whole set of data over these angular extents. Equation 2 gives the pixel resolutions of around 0.4 mm in azimuth and 0.6 mm in elevation. The THz image reveals a variety of different scattering features. The wheels, the treads, the main gun, the machine gun, and the snorkel are easily distinguished, as well as many other small features. This system simulates Ka-band radar data at 33 GHz.
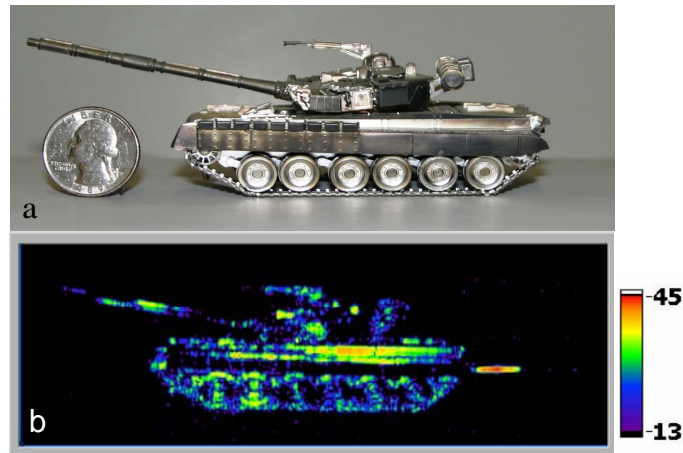

Figure 5. (a) photograph of 1/72nd scale model of a T-80BV tank, (b) 2.4 THz Azimuth/Elevation imagery of the scale model tank with pixel resolution of about 0.4x0.6 mm. A calibration object is located to the right of the image.

Coherent data processing provides significant signal-to-noise (S/N) enhancement in the imagery. To illustrate, the dihedron alone was placed in the target region and the backscattered signal was measured by the receiver. A 15 dB S/N ratio was measured from a spectrum analyzer trace, with the analyzer set at a 1 kHz resolution bandwidth. After imaging the target and dihedron (the bright spot to the right of the tank image in Fig. 5b) the S/N of the dihedron increased to 72 dB. The S/N should increase linearly with time, which for a typical 40 min scan implies an improvement of approximately 63 dB, in reasonable agreement with the measured gain of 57 dB. The 72 dB of signal-to-noise ratio implies that the receiver can detect the backscatter from 2.9 mm diameter sphere with a S/N of 10.

Figure 6a shows a photograph of a 4 inch square aluminum plate with raised 3 mm wide letters "STL" and the grooved 1.3 mm wide letters in the words "University of Massachusetts Lowell" and "Submillimeter-Wave Technology Laboratory" wrapped along a circle above and below the center. A 2.4 THz az/el image of the plate is shown in Fig. 6b. The amplitude values in dB are represented in colors on a linear color scale. The data were recorded from -1.8º to 4º elevations and from -4.8º to 4.8º azimuth with an angular spacing of 0.028º in elevation and 0.02º in azimuth. The pixel resolutions are around 0.4 mm in azimuth and 0.6 mm in elevation. "STL" letters can be easily seen and even 0.4 mm wide fabrication lines on the letters' surface are resolved. However, since the FWHM of the two-way beam was about 2.5 inches, which is less than the plate size, the edges of the plate were not illuminated sufficiently to generate a good signal-to-noise ratio. As a result, the smaller letters on the circular pattern of words are barely discernable.
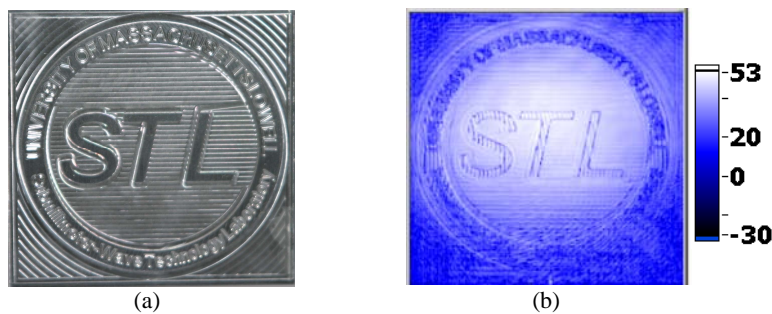

Fig. 6. (a) photograph of a metal plate with raised lettering, (b) 2.4 THz image of the plate.

If even higher resolution images are required, then larger integrated angles would have to be applied. However, it may cause image blurriness. The principal reason for this blurring effect lies in the approximation that a scatterer moves along a linear segment when rotated, instead of a circular segment. When large integrated angles are used, then this approximation is no longer valid, especially for scatterers far from the axis of rotation, and a synthetic aperture focusing technique[25] has to be applied to compensate for motion of a scatterer perpendicular to the direction of beam propagation.

To demonstrate that the 1.3 mm wide letters positioned closer to the axis of rotation can be resolved with the present system images of a 2009 Boston Marathon medal were generated. Figure 7a shows a photograph of the 2 inch diameter medal and Figure 7b demonstrates a 2.4 THz az/el image. The amplitude values in dB are represented in colors on a linear color scale.
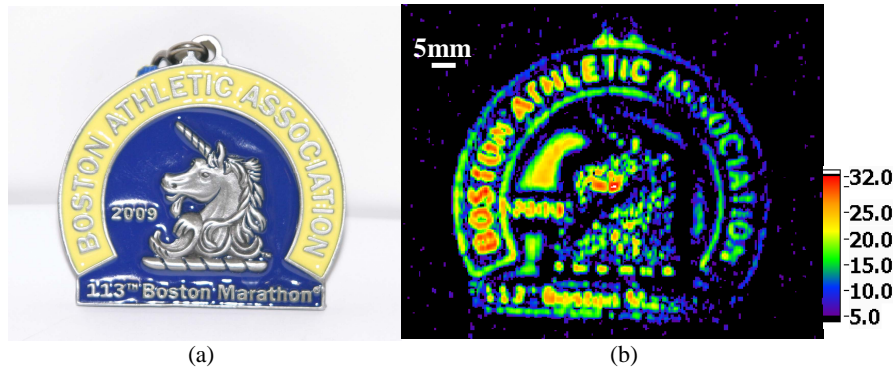

(a)   (b)

Figure 7. (a) photograph of the Boston Marathon medal, (b) 2.4 THz image of the medal.

The words "Boston Athletic Association" and the unicorn are well-resolved. However, the words "113 Boston Marathon" which have letters' width of 0.5 mm are still blurred.

5. Conclusions

In this work, for the first time, the operational frequency of coherent transceivers was extended to 2.4 THz and a THz quantum cascade laser (QCL) was implemented as a transmitter. A CO_2 laser-pumped molecular laser was used as a local oscillator and Schottky diodes as mixers. The QCL was frequency-locked to the LO to achieve a required phase stability for a coherent transceiver. Replacement of molecular laser sources by QCLs would greatly reduce complexity, cost, and size of coherent THz systems. As a demonstration of coherent transceiver capability, 2.4 THz images of several objects were produced using ISAR techniques, where a fixed position transceiver was used while an object was rotated in a precise motion in azimuth and elevation. Post-detection two dimensional FFT over an angular window formed the two dimensional high-resolution THz images. Submillemeter resolution was achieved.

References

[1] Sinclair, G., "Theory of models of electromagnetic systems," Proceedings of IRE, Vol. 36, No. 11, 1364-1370 Nov (1948).
[2] Coulombe, M. J., Horgan, T., and Waldman, J., Neilson, J., Carter, S., and Nixon, W., "A 160 GHz Polarimetric Compact Range for Scale Model RCS Measurements," Antenna Measurements and Techniques Association (AMTA) Proceedings, Seattle, WA, p. 239, October (1996).
[3] Coulombe, M. J., Horgan, T., and J. Waldman, Szatkowski, G., and Nixon, W., "A 520 GHZ Polarimetric Compact Range for Scale Model RCS Measurements," Antenna Measurements and Techniques Association (AMTA) Proceedings, Monterey, October (1999).
[4] Goyette, T. M., Dickinson, J. C., Waldman, J., Nixon, W. E., "Three Dimensional Fully Polarimetric W-band ISAR Imagery of Scale-Model Tactical Targets Using a 1.56 THz Compact Range," Proc. SPIE Vol. 5095, 66-74 Algorithms for Synthetic Aperture Radar Imagery X; Edmund G. Zelnio, Frederick D. Garber; Eds. September (2003).

[5] Waldman, J., Danylov, A. A., Goyette, T. M., Coulombe, M. J., Giles, R. H., Gatesman, A. J., Goodhue, W. D., Li, J., Linden, K. J., Nixon, W. E., "Prospects for quantum cascade lasers as transmitters and local oscillators in coherent terahertz transmitter/receiver systems" Proc. SPIE 7215 72150C (2009).

[6] Danylov, A. A., Goyette, T. M., Waldman, J., Coulombe, M. J., Gatesman, A. J., Giles, R. H., Goodhue, W. D., Qian, X., and Nixon, W. E., "Frequency stabilization of a single mode terahertz quantum cascade laser to the kilohertz level", Optics Express, Vol. 17, Issue. 9, 7525-7532 (2009).

[7] Barbieri, S., Alton, J., Baker, C., Lo, T., Beere, H., and Ritchie, D., "Imaging with THz quantum cascade lasers using a Schottky diode mixer," Opt. Express 13, 6497-6503 (2005).

[8] Darmo, J., Tamosiunas, V., Fasching, G., Kröll, J., Unterrainer, K., Beck, M., Giovannini, M., Faist, J., Kremser, C., and Debbage, P., "Imaging with a Terahertz quantum cascade laser," Opt. Express 12, 1879-1884 (2004).

[9] Chamberlin, D. R., Robrish, P. R., Trutna, W. R., Scalari, G., Giovannini, M., Ajili, L., and Faist, J., "Imaging at 3.4 THz with a quantum-cascade laser," Appl. Opt. **44**, 121-125 (2005).

[10] Nguyen, K. L., Johns, M. L., Gladden, L., Worrall, C. H., Alexander, P., Beere, H. E., Pepper, M., Ritchie, D. A., Alton, J., Barbieri, S., and Linfield, E. H., "Three-dimensional imaging with a terahertz quantum cascade laser," Opt. Express **14**, 2123-2129 (2006).

[11] Lee, A. W. M., Qin, Q., Kumar, S., Williams, B. S., and Hu, Q., "Real-time terahertz imaging over a standoff distance (> 25 meters)," Appl. Phys. Lett. 89, 141125 (2006).

[12] Behnken, B. N., Karunasiri, G., Chamberlin, D. R., Robrish, P. R., and Faist, J., "Real-time imaging using a 2.8 THz quantum cascade laser and uncooled infrared microbolometer camera," Opt. Lett. **33**, 440-442 (2008).

[13] Mensa, D.L., [High Resolution Radar Cross-Section Imaging], Artech House, (1991).

[14] Dickinson, J. C., Goyette, T. M., Waldman, J., "High Resolution Imaging using 325GHz and 1.5THz Transceivers," Fifteenth International Symposium on Space Terahertz Technology (STT2004), Northampton, MA, April 27-29, (2004).

[15] Henry, C., "Theory of the linewidth of semiconductor lasers," IEEE J. of Quantum Electronics, Vol. 18, Issue 2, 259 – 264 (1982).

[16] Weidmann, D., Joly, L., Parpillon, V., Courtois, D., Bonetti, Y., Aellen, T., Beck, M., Faist, J., and Hofstetter, D., "Free-running 9.1-µm distributed-feedback quantum cascade laser linewidth measurement by heterodyning with a $C^{18}O_2$ laser," Opt. Lett. **28**, 704-706 (2003).

[17] Green, R. P., Xu, J.-H., Mahler, L., Tredicucci, A., Beltram, F., Giuliani, G., Beere, H. E., and Ritchie, D. A., "Linewidth enhancement factor of terahertz quantum cascade lasers," Appl. Phys. Lett. 92, 071106 (2008).

[18] Betz, A. L., Boreiko, R. T., Williams, B. S., Kumar, S., Hu, Q., and Reno, J.L., "Frequency and phase-lock control of a 3 THz quantum cascade laser", Opt. Lett., Vol. 30, 1837-1839 (2005).

[19] Baryshev, A., Hovenier, J. N., Adam, A. J. L., Kasalynas, I., Gao, J. R., Klaassen, T. O., Williams, B. S., Kumar, S., Hu, Q., and Reno, J.L., "Phase locking and spectral linewidth of a two-mode terahertz quantum cascade laser," Appl. Phys. Lett., Vol. 89, 031115 (2006).

[20] Rabanus, D., Graf, U. U., Philipp, M., Ricken, O., Stutzki, J., Vowinkel, B., Wiedner, M. C., Walther, C., Fischer, M., and Faist, J., "Phase locking of a 1.5 Terahertz quantum cascade laser and use as a local oscillator in a heterodyne HEB receiver," Opt. Express 17, 1159-1168 (2009).

[21] Khosropanah, P., Baryshev, A., Zhang, W., Jellema, W., Hovenier, J. N., Gao, J. R., Klapwijk, T. M., Paveliev, D. G., Williams, B. S., Kumar, S., Hu, Q., Reno, J. L., Klein, B., and Hesler, J. L., "Phase locking of a 2.7 THz quantum cascade laser to a microwave reference," Opt. Lett. 34, 2958-2960 (2009).

[22] Richter, H., Semenov, A. D., Pavlov, S. G., Mahler, L., Tredicucci, A., Beere, H. E., Ritchie, D. A., Il'in, K. S., Siegel, M., and Hübers, H.-W., "Terahertz heterodyne receiver with quantum cascade laser and hot electron bolometer mixer in a pulse tube cooler," Appl. Phys. Lett. 93, 141108 (2008).

[23] Danylov, A. A., Waldman, J., Goyette, T. M., Gatesman, A. J., Giles, R. H., Linden, K. J., Neal, W.R., Nixon, W.E., Wanke, M. C., and Reno, J. L., "Transformation of the multimode terahertz quantum cascade laser beam into a Gaussian, using a hollow dielectric waveguide", Applied Optics, Vol. 46, Issue 22, 5051-5055 (2007).

[24] Danylov, A. A., Waldman, J., Goyette, T. M., Gatesman, A. J., Giles, R. H., Li, J., Goodhue, W. D., Linden, K. J., and Nixon, W. E., "Terahertz sideband-tuned quantum cascade laser radiation," Opt. Express, Vol. 16, 5171-5180 (2008).

[25] Reference 13, Chapter 5.